Adaptive Electronic Equalization for Non-Ideal Optical Coherent Receivers

A. Vgenis[1], C. S. Petrou[1], I. Roudas[1], I. Chochliouros[2], G. Agapiou[2] and T. Doukoglou[2]
[1]Univ. of Patras, Dept. of Electrical and Computer Engineering, Patras, Greece, [2]OTE S.A., Athens, Greece
E-mail: [1]{vgenis, petrou, roudas}@ece.upatras.gr, [2]{ichochliouros, gagapiou, tdoukoglou}@oteresearch.gr

***Abstract*—In coherent optical systems, apart from fiber chromatic dispersion and polarization mode dispersion, transmitter and local oscillator phase noise and intermediate frequency offset also have a significant impact on the system's performance. We study, by simulation, the performance of adaptive equalization, assisted by a recursive phase noise-removing unit, on the combined impact of the above effects. An intermediate frequency offset larger than 300 MHz induces an SNR penalty over 6 dB, whereas the system's tolerance over phase noise is larger, allowing for the use of lasers with linewidth equal to almost 30 MHz, with less than 4 dB penalty.**

I. INTRODUCTION

Chromatic dispersion (CD) and polarization mode dispersion (PMD) have a significant impact on the performance of optical systems as data rates increase [1], [2]. Instead of using expensive and bulky optical equalization methods [3] for their compensation, coherent detection, in conjunction with adaptive electronic equalization, can be employed [4]. Adaptability is essential due to the time-variant nature of PMD and possible changes in fiber length caused by optical switching in all-optical networks. Due to the phase preservation property of coherent receivers, adaptive electronic equalization is, in principle, capable of removing linear fiber impairments with zero total penalty. However, coherent homodyne detection suffers from intermediate frequency (IF) offset, which varies very slowly with time and normally requires automatic frequency control (AFC) in order to be removed. In addition, for optical communication systems using phase modulation and coherent detection, phase noise (PN) causes additional performance degradation [1]. Experimental and theoretical studies have been published [5]-[9] that demonstrate the performance of adaptive electronic equalization against CD and PMD in optical coherent systems. However, to our knowledge, the impact of IF offset on the performance of these equalizers has not yet been examined. Most theoretical studies assume ideal homodyne detection [5], [6]. Most experimental studies either manage to keep IF offset under strict limits [7], or use complex, off-line methods for removing it [8], [9].

In this article, we study, by computer simulation, the performance of an adaptive electronic equalizer against the combined effect of CD and PMD, in the presence of phase noise and, for the first time, of the IF offset generated by free running transmitter and local oscillator lasers. The receiver under study is equipped with an additional digital signal processing application-specific integrated circuit (DSP ASIC) for the removal of phase noise [5] symbol-by-symbol. It can operate with up to 300 MHz of IF offset and phase noise generated by wide-linewidth lasers, combined with CD and PMD.

The rest of the paper is organized as follows. In section II, we describe the simulated system. In section III, the simulation models of the optical fiber, the coherent receiver, and the electronic equalizer are presented. Simulation results are shown in section IV. Conclusions are presented in section V.

II. SYSTEM OVERVIEW

The system under study is shown in Fig. 1. Four pseudo-random bit sequences (PRBS 1-4), at a bit rate R_b each, are differentially encoded (DE) and transformed into non-return-to-zero (NRZ) pulse sequences, which externally modulate the output of the transmitting laser diode, using two quadrature modulators. Two optical differential quadrature phase shift keying (DQPSK) signals are produced, at a symbol rate $R_s = R_b$ each. The two signals are added together using a polarization beam combiner to form a polarization-multiplexed DQPSK (PM-DQPSK) signal which is transmitted into the optical fiber. The optical fiber is characterized by CD, PMD and attenuation. Optical amplifiers, placed after each fiber span, are used to compensate for the optical fiber's attenuation. After optical bandpass filtering, the distorted

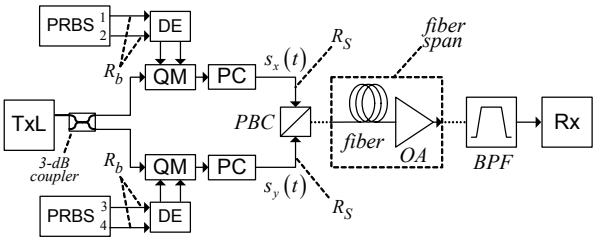

Figure 1. System block diagram (Symbols: PRBS: Pseudo-random bit sequence, DE: Differential encoding, TxL: Transmitter laser, QM: Quadrature modulator, PC: Polarization controller, PBC: Polarization beam combiner, OA: Optical amplifier, BPF: Optical bandpass filter, Rx: Coherent receiver, s : Transmitted signal, x, y : Orthogonal states of polarization (SOP), R_b : Bit rate, R_s : Symbol rate).

978-1-4244-1876-3/08/$25.00 ©2008 IEEE

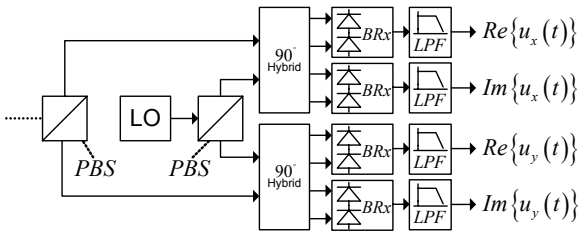

Figure 2. Receiver front end (Symbols: LO: Local oscillator, PBS: Polarization beam splitter, BRx: Balanced receiver, LPF: Low-pass filter, u : Filtered analog electrical signal).

waveform is demodulated using a phase- and polarization-diversity homodyne coherent receiver. Initially, at the receiver front end, the received signal is split into two arbitrary orthogonal states of polarization and combined with the light of the local oscillator in two 2×4 90° optical hybrids, as illustrated in Fig. 2. The signals at the optical hybrids' outputs are detected by four balanced detectors. The four electrical waveforms produced correspond to the in-phase and quadrature components of x and y polarizations, respectively. After low-pass filtering (LPF), the analog waveforms are fed into the DSP section of the receiver, which is pictured in Fig. 3. There, initially, sampling and analog-to-digital conversion take place. Then, the samples of the quadrature components are processed so that fiber-induced distortion is compensated for and the combined phase shift due to phase noise and IF offset is removed, to a certain extent. Distortion compensation is achieved via a linear, fractionally-spaced equalizer. Tap spacing is set to half the symbol period T, which requires two-fold oversampling. A $T/2$-spaced equalizer has superior spectral characteristics and increased tolerance of sampling phase errors in comparison with the T-spaced equalizer [4], [10]. It also exhibits at least similar performance to the decision feedback equalizer (DFE) [5], [6], [10] in coherent optical systems, but with reduced complexity. The number of equalizer L taps is a design parameter and its role will be discussed below.

III. Theoretical Model

In this section, we describe the fiber-induced distortions, the modeling of additive noise, phase noise and IF offset. We also describe the structure and operation of the equalizer and the DSP unit that removes phase noise and IF offset.

The transmitted waveforms $s_x(t)$, $s_y(t)$ for the two orthogonal polarizations can be written, in equivalent baseband notation [10], as

$$\begin{aligned} s_{x,y}(t) &= \mathrm{A} e^{j\theta_t(t)} \sum_{k=1}^{M} e^{j\varphi_{x,y}^k} g(t-kT) \\ &= e^{j\theta_t(t)} z_{x,y}(t) \end{aligned} \quad (1)$$

where A is the carrier amplitude, $\theta_t(t)$ is the transmitter phase noise, $\varphi_{x,y}^k$ is the transmitted phase for each orthogonal polarization, corresponding to the k – th symbol, M is the length of the transmitted sequence of symbols, and $g(t)$ is the symbol shape, which is assumed to be ideal NRZ. With $z_{x,y}(t)$ we denote the phase noise-free optical waveforms.

Phase noise is caused by random frequency fluctuations of the transmitting and local oscillator lasers [1]. It is modeled as a Wiener-Lévy process [11]. The phase noise is generated by the transmitting laser and is sent through the optical fiber. We assume that optical filtering by the fiber and the optical bandpass filter (BPF) does not affect the statistics of the transmitting laser phase noise. Additional phase noise is generated by the local oscillator at the receiver.

The optical signal is fed into the optical fiber, which is assumed to be linear, exhibiting only CD and PMD. The optical fiber's transfer function has the form of a 2×2 matrix (in equivalent baseband notation [10]):

$$\mathbf{H}(f) = \mathbf{J}(f) e^{j\pi^2 \gamma \left(\frac{f}{R_S}\right)^2}. \quad (2)$$

In (2) we use boldface letters to denote matrices and vectors. More specifically, $\mathbf{J}(f)$ denotes the 2×2 Jones matrix of the optical fiber, including polarization rotations and all PMD orders [12], f is the frequency deviation from the carrier frequency and γ is the CD index [13], given by

$$\gamma = \frac{1}{\pi} R_S^2 L_{fiber} D(\lambda) \frac{\lambda^2}{c}, \quad (3)$$

where L_{fiber} is the fiber's length, λ is the carrier wavelength and $D(\lambda)$ is the chromatic dispersion parameter [1]. We ignore higher-order CD, polarization dependent loss and fiber non-linearities.

The impulse response of the optical fiber also has a matrix-form

$$\mathbf{h}(t) = \mathcal{F}^{-1}\{\mathbf{H}(f)\} = \begin{bmatrix} h_{11}(t) & h_{12}(t) \\ h_{21}(t) & h_{22}(t) \end{bmatrix}, \quad (4)$$

where the operator $\mathcal{F}^{-1}\{.\}$ denotes the inverse Fourier transform.

We assume that the optical BPF has an ideal rectangular transfer function, with bandwidth much larger than the signal bandwidth, so we ignore its impact on the signal. After detection, the two analog complex signals $r_x(t)$ and $r_y(t)$, for the two polarizations, respectively, can be written as:

$$\begin{aligned} r_x(t) &= B e^{j\theta(t)} \left[h_{11}(t) \otimes z_x(t) + h_{12}(t) \otimes z_y(t) \right] \\ &\quad + n_x(t) \\ r_y(t) &= B e^{j\theta(t)} \left[h_{21}(t) \otimes z_x(t) + h_{22}(t) \otimes z_y(t) \right] \\ &\quad + n_y(t) \end{aligned} \quad (5)$$

.

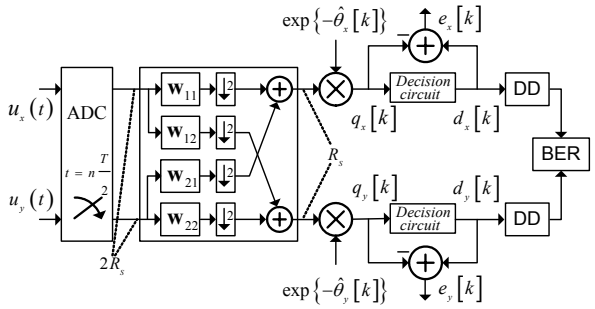

Figure 3. Block diagram of the receiver DSP unit (Symbols: ADC: Analog-to-digital converter, **w**: Transversal filter impulse response, $\hat{\theta}$: Phase noise estimate, q, d: Decision circuit input and output, e: error signal, DD: Differential decoding, BER: Bit error rate counter).

In (5), we used the following symbols: The multiplicative coefficient B denotes the amplitude of the detected electrical waveforms. The phase component $\theta(t)$ is given by $\theta(t) = \omega_{IF}(t)t + \theta_N(t)$, where $\theta_N(t)$ denotes the total phase noise, i.e., the sum of the phase noises from the transmitter and the local oscillator, and $\omega_{IF} = 2\pi f_{IF}$ is the angular intermediate frequency, with f_{IF} being the IF offset. The IF offset is defined as the difference between the signal's carrier and the LO's frequencies. Due to laser frequency drift, perfect homodyne detection is not feasible and a difference between the two frequencies always exists. The total phase noise of the IF photocurrent is quantitatively characterized by the 3-dB IF linewidth $\Delta\nu_{IF} = \Delta\nu_{Tx} + \Delta\nu_{LO}$, where $\Delta\nu_{Tx}$, $\Delta\nu_{LO}$ are the transmitter's and LO's linewidths, respectively [1]. In (5), $n_x(t)$ and $n_y(t)$ describe the sum of all additive noises that affect each polarization. In the optical domain, the signal is contaminated with amplified spontaneous emission (ASE) noise from optical amplifiers. In the electrical domain, shot and thermal noise are introduced by the photodiodes and receiver circuitry, respectively. ASE and thermal noise can be modeled in equivalent baseband notation as Gaussian complex random variables, while shot noise follows a Poisson distribution [1]. For high levels of optical power, shot noise may be also approximated by a Gaussian distribution [1]. Consequently, we can model the combined effect of ASE, shot and thermal noises, as two independent, equivalent complex additive white Gaussian (AWGN) noise sources, one for each polarization.

The detected signals are filtered by electronic LPFs, that have an impulse response $h_e(t)$ and produce the waveforms $u_{x,y}(t) = h_e(t) \otimes r_{x,y}(t)$, for the two polarizations, respectively. We assume that phase noise and IF offset are not affected by lowpass filtering.

After two-fold oversampling compared to the symbol rate, two samples of $u_{x,y}(t)$ per symbol period T enter the equalizer, which compensates for the effect of CD and PMD. The block diagram of the electronic equalizer and the assisting signal processing mechanisms is shown in Fig. 3. It consists of four complex-valued transversal filters with impulse responses $\mathbf{w}_{11}, \mathbf{w}_{12}, \mathbf{w}_{21}, \mathbf{w}_{22}$ of length L, arranged in a butterfly structure [5], [9]. The equalizer implements a 2×2 matrix impulse response similar to the structure of the fiber's one, symbolized by $\mathbf{W}$, where $\mathbf{w}_{11}, \mathbf{w}_{12}, \mathbf{w}_{21}, \mathbf{w}_{22}$ serve as elements in the equalizer matrix impulse response. The equalizer generates one sample per symbol, at time instants kT, $k \in \mathbb{Z}$.

If the fiber's transfer function is known and constant, the equalizer's tap weights can be appropriately selected, in order to invert the product of the LPF and the optical fiber's transfer functions, i.e., $\mathcal{F}\{h_e(t)\}\mathbf{H}(f)$. However, the transfer function $\mathbf{H}(f)$ includes the effect of time-varying PMD. In addition, the optical fiber's length is not always constant and a-priori known in the case of reconfigurable all-optical networks. Consequently, an adaptive method must be used for tap-weight adjustment. The least mean squares (LMS) [10] algorithm is used to control the equalizer's tap weights, following the minimum mean-square error (MMSE) criterion [10]. The tap weight adjustment is described by the equation

$$\mathbf{W}[k+1] = \mathbf{W}[k] + \mu \mathbf{u}^*[k]\mathbf{e}^T[k]\hat{\mathbf{\Theta}}[k], \quad (6)$$

where we use the notation $a[k] = a(kT)$, $k \in \mathbb{Z}$, for the representation of discrete time signals. In (6), $\mathbf{u}[k] = [\mathbf{u}_x[k] \quad \mathbf{u}_y[k]]^T$ and contains the L-sized line vectors $\mathbf{u}_x[k]$, $\mathbf{u}_y[k]$, each made from the L last output samples of the sampling circuit, for each polarization, respectively, μ denotes the LMS step size,

$$\mathbf{e}[k] = \begin{bmatrix} d_x[k] - q_x[k] \\ d_y[k] - q_y[k] \end{bmatrix} \quad (7)$$

is a vector that contains the error sample, i.e., the difference between the output and the input samples of the decision circuit for each polarization, stars denote complex conjugates and the matrix

$$\hat{\mathbf{\Theta}}[k] = \begin{bmatrix} e^{j\hat{\theta}_x[k]} & 0 \\ 0 & e^{j\hat{\theta}_y[k]} \end{bmatrix} \quad (8)$$

is used for stability reasons [5]. Phases $\hat{\theta}_{x,y}[k]$ are the estimates of the phase error caused by phase noise and IF offset, for every sample at time instant kT, $k \in \mathbb{Z}$, in both polarizations. These estimates are calculated using the phase shift between the samples at the input and the output of the decision circuit at time instants

$(k-1)T$, $k \in \mathbb{Z}$ [5]:

$$\hat{\theta}_{x,y}[k] = \hat{\theta}_{x,y}[k-1] + \delta \arg\left\{q_{x,y}[k-1]\, d^{*}_{x,y}[k-1]\right\}, \quad (9)$$

where $q_{x,y}[k]$, $d_{x,y}[k]$ are the samples for each state of polarization at the input and the output of the decision circuit, respectively, and $\delta \in [0,1]$ is the step size parameter for the phase noise cancellation algorithm. The estimates $\hat{\theta}_{x,y}[k]$ are subtracted from the phase of the samples at the output of the equalizer, as shown in Fig. 3. This symbol-by-symbol phase noise estimating and removing circuitry is simpler to implement than the block based signal processing methods that are usually used in the literature, including FFT [9] or rise of the complex symbols to the fourth power [8], [14].

Finally, the estimates of the transmitted symbols are differentially decoded (DD) and compared to the corresponding PRBS at the transmitter for bit error rate (BER) calculations.

IV. Simulation Results

We simulate a system using a standard single mode fiber (SMF) with CD parameter D=16 ps/nm/km at 1550 nm. The bit rate is R_b=10 Gb/s, so the respective symbol rate is R_S=10 GBd per polarization. First-order PMD exclusively is considered for all simulations, with DGD ranging from $0.2T$ to $2.5T$. The relative angle between the fiber's PSP's and the two orthogonal transmitted states of polarization is equal to 45° (worst case scenario). The electronic LPF has a 3-dB bandwidth equal to 8 GHz. Step size parameters μ, δ are set to the values 0.001 and 0.5, respectively, optimized for stability of the recursive algorithms and low BER. For the purposes of the simulations we consider a single-span fiber-optic communication system with variable length, followed by a single optical amplifier, which fully compensates for the fiber's attenuation. The SNR is set by appropriately selecting the power of the optical signal at the input of the optical amplifier, which has a fixed gain and a noise figure of 4 dB. The SNR penalty is calculated for BER 10^{-3}, which can be reduced to 10^{-15} using forward error correction (FEC) [8]. The SNR penalty for each case is calculated by comparing the SNR after transmission to the required SNR for BER=10^{-3} for the back-to-back case, for an ideal homodyne configuration with zero laser 3-dB linewidth and an equalizer with 50 taps. BER is calculated using Monte Carlo simulations. Non-linear effects have been neglected.

Fig. 4 shows constellation diagrams at the input of the electronic equalizer and at the output of the phase noise removing circuit. In order to demonstrate the system's performance against phase noise and IF offset we consider three case studies. In diagrams (a) and (b), only phase noise is simulated ($\Delta\nu_{IF}$=2 MHz), while CD, PMD, and IF offset are set to zero. In (c), (d), CD, PMD, $\Delta\nu_{IF}$ are set to zero and IF offset of 100 MHz is simulated. Finally, in (e), (f), $\Delta\nu_{IF}$=2 MHz, IF offset is 100 MHz, γ=1.2 and PMD is set as described earlier with DGD equal to $0.2T$. To facilitate visualization, additive noise has been omitted. It is observed that the equalizer manages to restore the constellation diagrams to, almost point-like form, in all cases.

Fig. 5 shows the impact of the number of filter taps on the performance of the electronic equalizer. An IF offset of 100 MHz and a $\Delta\nu_{IF}$ equal to 10 MHz are assumed. The SNR penalty for BER=10^{-3} is calculated, as a function of γ, for an electronic equalizer with 8, 14, 22 and 50 taps, respectively. Results are shown for DGD= $0.2T$ and DGD= $2.5T$. It is observed, that even for the back-to-back case, due to phase noise and IF offset, the SNR penalty is non-zero. For DGD= $0.2T$, it can be seen that the equalizers with 8 and 14 taps can maintain the target BER for values of γ up to 1 and 2, respectively, with SNR penalty less than 3 dB. The equalizer with 22 taps gives less than 3 dB penalty for γ about 3.5. If the length of the equalizer is increased to 50 taps, the penalty remains below 2 dB for γ up to 5. In the extreme case

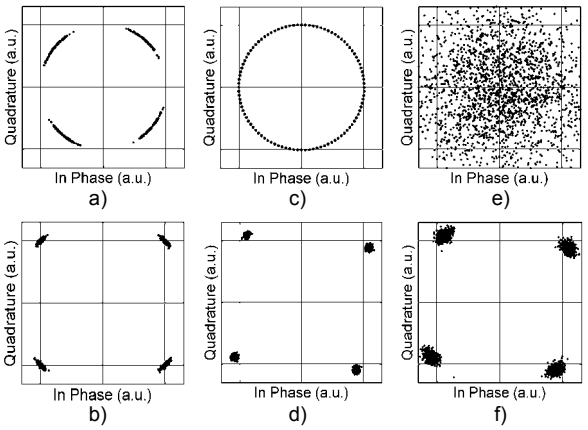

Figure 4. Equalizer input (upper row) and decision circuit input (lower row) constellation diagrams. ((a)-(b): phase noise only, (c)-(d): IF offset only, (e)-(f): CD, PMD, phase noise, IF offset).

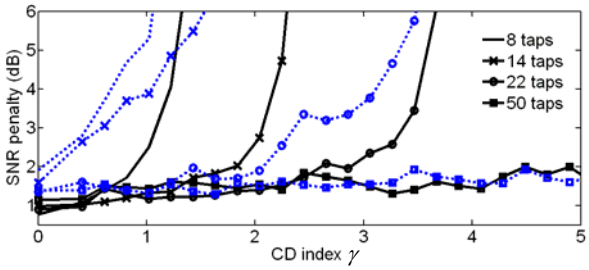

Figure 5. SNR penalty vs. CD index γ for various equalizer transversal filter lengths. Conditions: f_{IF}=100 MHz, $\Delta\nu_{IF}$=10 MHz (solid line: DGD= $0.2T$, dotted line: DGD= $2.5T$).

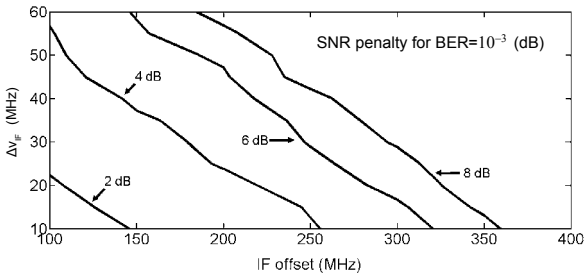

Figure 6. Contour plot of SNR penalty for BER=10^{-3} vs IF offset and $\Delta\nu_{IF}$. CD index γ is 2.

when DGD= $2.5T$, we observe that the equalizers with 8 and 14 taps fail to maintain the SNR penalty below 3 dB for values of γ greater than 0.5. The equalizer with 22 taps manages to reach γ slightly over 2 with SNR penalty less than 3. If the length of the equalizer is again increased to 50 taps, the system is resilient to this increase of DGD and maintains the SNR penalty below 2 dB for the whole range of γ studied here. It can be seen that for the removal of distortion caused by DGD up to $2.5T$, more than 14 taps are necessary. The equalizer with 22 taps is capable of compensating for PMD up to $2.5T$ but is limited by CD, while the equalizer with 50 taps is not influenced by PMD and can, additionally, equalize for any amount of CD studied here.

The combined impact of phase noise and IF offset on the performance of the system with γ=2, using an equalizer with 22 taps, is presented in the contour plot of Fig. 6. We have calculated the SNR penalty for BER=10^{-3} for different values of $\Delta\nu_{IF}$ and IF offset. As expected, there is a trade-off between $\Delta\nu_{IF}$ and IF offset. With this system, even lasers with very wide linewidth can be used, if IF offset is limited to low values. Conversely, the use of low-linewidth lasers could relax the requirements on IF offset control.

V. CONCLUSIONS

We demonstrate the impact of IF offset on the performance of a coherent homodyne system, employing electronic equalization against CD and PMD and additional signal processing against phase noise. The system can operate with a SNR penalty less than 6 dB with IF offset up to 300 MHz if narrow-linewidth lasers are used. If IF offset is kept below 150 MHz, wide-linewidth lasers can be used giving the same SNR penalty.

ACKNOWLEDGMENT

This work is sponsored by the grant 05NON-EU-552 from the Greek Development Ministry.

REFERENCES

[1] G. P. Agrawal, *Fiber-Optic Communication Systems*, 3rd ed. New York: Wiley, 2002.

[2] H. Kogelnik, R. M. Jopson, and L. E. Nelson, "Polarization-mode dispersion," in *Optical Fiber Telecommunications IVB*, I. P. Kaminow and T. Li, Eds., San Diego: Academic Press, 2002.

[3] T. Nielsen and S. Chandrasekhar, "OFC 2004 workshop on optical and electronic mitigation of impairments," *J. Lightw. Technol.*, vol. 23, no. 1, pp. 131–142, Jan. 2005.

[4] J. H. Winters and R. Gitlin, "Electrical signal processing techniques in long-haul fiber-optic systems," *IEEE Trans. Commun.*, vol. 38, pp. 1439–1439, Sept. 1990.

[5] D. E. Crivelli, H. S. Carter, and M. R. Hueda, "Adaptive digital equalization in the presence of chromatic dispersion, PMD, and phase noise in coherent fiber optic systems," in *IEEE Global Telecommun. Conf. (GLOBECOM)*, Dallas, TX, 2004, vol. 4, pp. 2545–2551.

[6] B. Spinnler, P. M. Krummrich, and E. -D. Schmidt, "Chromatic dispersion tolerance of coherent optical communications systems with electrical equalization," in *Optical Fiber Communications Conf. (OFC 2006),* Anaheim, CA, Mar. 2006, Paper OWB2.

[7] S. Tsukamoto, K. Katoh, and K. Kikuchi, "Unrepeated transmission of 20-Gb/s optical quadrature phase-shift-keying signal over 200-km standard single-mode fiber based on digital processing of homodyne-detected signal for group-velocity dispersion compensation," *IEEE Photon. Technol. Lett.*, vol.18, no.9, pp. 1016–1018, May 2006.

[8] C. R. S. Fludger, T. Duthel, T. Wuth, and C. Schulien, "Uncompensated transmission of 86 Gbit/s polarization multiplexed RZ-QPSK over 100 km of NDSF employing coherent equalization," in *Proc. ECOC*, Cannes, France, Sept. 2006, Postdeadline Paper Th.4.3.3.

[9] S. J. Savory, G. Gavioli, R. I. Killey, and P. Bayvel, "Electronic compensation of chromatic dispersion using a digital coherent receiver," *Optics Express*, vol. 18, no. 5, pp. 2120–2126, Mar. 2007.

[10] J. G. Proakis, *Digital Communications*, 4th ed. New York: McGraw-Hill, 2001.

[11] J. Salz, "Modulation and detection for coherent lightwave communications," *IEEE Commun. Mag.*, vol. 24, no. 6, pp. 38–49, June 1986.

[12] C. D. Poole and J. Nagel, "Polarization effects in ligthwave systems," in *Optical Fiber Telecommunications IIIA*, I. P. Kaminow and T. L. Koch, Eds., San Diego: Academic Press, 1997.

[13] A. F. Elrefaie, R. E. Wagner, D. A. Atlas, and D. G. Daut, "Chromatic dispersion limitations in coherent ligthwave transmission systems," *J. Lightw. Technol.*, vol. 6, no. 5, pp. 704–709, May 1988.

[14] A. J. Viterbi and A. M. Viterbi, "Nonlinear estimation of PSK-modulated carrier phase with application to burst digital transmission," *IEEE Trans. Inf. Theory*, vol. IT-29, pp. 543–551, July 1983.